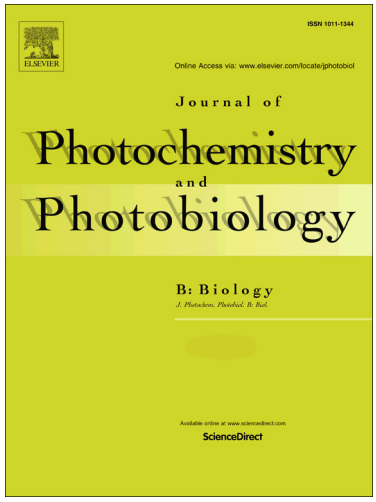

Ferrocene incorporated selenoureas as anticancer agents

Raja Azadar Hussain, Amin Badshah, John M. Pezzuto, Nadeem Ahmed, Tamara P. Kondratyuk, Eun-Jung Park

PII: S1011-1344(15)00147-5
DOI: http://dx.doi.org/10.1016/j.jphotobiol.2015.04.024
Reference: JPB 10021

To appear in: *Journal of Photochemistry and Photobiology B: Biology*

Received Date: 26 February 2015
Revised Date: 17 April 2015
Accepted Date: 20 April 2015

Please cite this article as: R.A. Hussain, A. Badshah, J.M. Pezzuto, N. Ahmed, T.P. Kondratyuk, E-J. Park, Ferrocene incorporated selenoureas as anticancer agents, *Journal of Photochemistry and Photobiology B: Biology* (2015), doi: http://dx.doi.org/10.1016/j.jphotobiol.2015.04.024

Ferrocene incorporated selenoureas as anticancer agents

Raja Azadar Hussain[*1], Amin Badshah[1], John M. Pezzuto[2], Nadeem Ahmed[2,3], Tamara P. Kondratyuk[2] and Eun-Jung Park[2]

1. Co-ordination Chemistry Laboratory, Department of Chemistry, Quaid-i-Azam University 45320, Islamabad, Pakistan.
2. University of Hawaii at Hilo.
3. Phytoharmone Laboratory, Department of Plant Sciences, Quaid-i-Azam University 45320, Islamabad, Pakistan.

Abstract

For a compound to be a best chemopreventive agent it should be a descent DNA binder and at the same time should be active against any of the three stages of carcinogenesis i.e. cancer initiation, cancer propagation and tumor growth. Most of the problems associated with chemotherapy can be overcome if the chemopreventive agent is active against all the three stages of cancer development. Cancer may be initiated by higher concentration of free radicals, inflammating agents and phase I enzymes (Cytochrome P450) in the body. Cancer propagation can be very efficiently controlled by inducing the phase II enzymes (glutathione S-transferases (GSTs), UDP-glucuronosyl transferases, and quinone reductases) in the body and cancer termination depends on the killing of the faulty cells i.e. cytotoxic actions. This article reports comprehensively the comparative DNA binding studies (with, cyclic voltammetry, UV-vis spectroscopy and viscometry), antioxidant activities (DPPH scavenging), anti-inflammatory activities (nitrite inhibition), phase I enzyme inhibition activities (aromatase inhibition), phase II enzyme induction studies (quinone reductase induction) and cytotoxic studies against

neuroblastoma (MYCN2 and SK-N-SH), liver cancer (Hepa 1c1c7) and breast cancer (MCF-7) of seventeen ferrocene incorporated selenoureas.

Key Words: Ferrocene incorporated selenoureas, enzyme inhibition and induction, antioxidant, anti-inflammatory, anticancer.

1. Introduction

Selenoureas are known for their free radical scavenging [1-6], enzyme inhibition [7-9], anticancer activities, and DNA binding potencies [10-14]. Historically, scientific community was reluctant of their use in bioorganic chemistry due to the presence of selenium which was considered to be an absolute biological poison those days [15]. It is evident from the fact that acylselenoureas were synthesized way back in 1937 [16] but the interest in their bioinorganic chemistry developed after the findings that selenium is present in the bacterial enzymes formate dehydrogenase and glycine reductase in 1971 [17]. Until now selenium derivatives have been evaluated for their applications as anti-infective drugs (antifungal, antibacterial and antiviral), photochemotherapeutic agents, antitumor agents, cytokine inducers/immunomodulators, enzyme inhibition (nitric oxide synthase inhibitors, inosine monophosphate dehydrogenase inhibitors, lipoxygenase inhibitors, urdpase and thymidylate synthase inhibitors, and tyrosine kinase and iodothyronine deiodinase inhibitors), antioxidant defense enzymes (reduction of hydroperoxides-GPx mimics, reduction of peroxinitriles, and lipid peroxidation), antihypertensive and cardiotonic agents [18]. But there are no reports available for the systematic anticancer studies of selenoureas which should start from activities against cancer initiation (antioxidant and anti-inflammatory activities with phase I enzyme inhibition), and end up with activities against cancer propagation (phase II enzyme induction) and tumors (cytotoxicity against cancer cell lines).

On the other end, ferrocene derivatives have shown their importance in the drug development. Earlier attempts on ferrocene derivatives for their biological applications were individualistic in nature and it was known in 1978 (compound 1) that they are active against lymphocytic leukemia P-388 [19] (Chart 1, compound 1-10). Other similar type of findings have shown the activity of ferrocene derivatives against lungs carcinoma (compound 2) [20], 70% tumor growth inhibition (compound 3) against Ca-755 cell lines [21] and 100% inhibition of solid (compound 4) tumor [22]. But detail studies have opened new horizons of research on ferrocene. Following are some important developments in this regard:

- Illudin M (compound 5a) (derived from mashroom) is active against prostate, ovarian, pancreatic, renal and breast cancer. Ferrocene incorporated Illudin M (compound 5b) has shown less toxicity for nonmalignant fibroblasts while more cancer selectivity and more cell line specificity than parent Illudin M. This improvement was partially attributed to the shielding of enone group by ferrocene due to the attack of glutathione [23].
- Ferrocene incorporated tamoxifen (compound 6b) has shown better activities than simple tamoxifen (compound 6a) against breast cancer cell line MCF-7 at a concentration of 1 μM [23-27].
- Ferrocene incorporated nilutamides (compound 7b) derivatives have shown enhanced activities than simple nilutamides (compound 7a) towards prostate cancer. Moreover this work suggested that the introduction of ferrocene has very similar effect, which was obtained by the introduction of an aromatic ring [28, 29].
- Raloxifens (compound 8a) have shown activities against ovarian, cervical, lung, colon and breast cancer cell lines. Incorporation of ferrocene to raloxifens (compound 8b) has

been reported to improve their cytotoxicity and one of the compounds have shown the activity which is even better than cis-platin [30].

- Ferrocene incorporated testosterone (compound 9b) and dihydrotestosterone (compound 10b) derivatives have shown better activities than simple testosterone (compound 9a) and dihydrotestosterone (compound 10a) depending upon the position at which ferrocene has been incorporated [26].
- For the research work presented in this article, introduction of ferrocene moiety was also necessary because of following reasons:
    - Ferrocene is a beautiful electrochemical and spectroscopic marker which enabled us to evaluate its biological applications (specially the DNA binding studies with cyclic voltammetry and UV-vis spectroscopy [1, 11-14, 31, 32]).
    - Because of its lipophilic character it can cross the blood brain barrier and several activities inside the cells can be performed very easily.
    - Moreover, it is nontoxic for the living organisms and its incorporation does not have any negative impact inside the living organisms.

Cancer may simply be defined as, uncontrolled proliferation of the cells which may be initiated by a change in the genetic makeup or DNA repair mechanism, propagated by the growing of the mutated cells and finally ends up with tumor growth [33]. A chemopreventive agent is any chemical compound which can prevent, block or reverse any of the three above mentioned stages of carcinogenesis. One of the most preliminary criterion for any anticancer agent is that, it should bind/interact with DNA [1]. Different compounds with different functionalities can bind with the DNA differently. Drug-DNA interactions are mainly of two types:

- Covalent binding
- Noncovalent binding

Covalent binding is generally exhibited by alkylating agents and intrastrand crosslinkers and is characterized by irreversible nature of interaction, complete inhibition of the cellular processes and cell death [34]. Noncovalent interactions are subdivided into external binding, intercalation and groove binding. They are generally reversible and only cause the conformational changes to interfere with normal DNA functions [35]. Different techniques are used for DNA binding studies which include cyclic voltammetry (CV), UV-vis spectroscopy, fluorimetry, laser light scattering and viscometry etc [31]. We have used CV for DNA binding studies of synthesized FIS, mainly because of their best electrochemical signals due to the presence of ferrocene. The results obtained from CV have been verified with UV-vis spectroscopy and viscometry.

Aerobically respirating organisms produce free radicals (superoxide, hydroxide, peroxynitrile etc.) during metabolism processes mainly in mitochondria which are considered responsible for Alzheimer's disease, myocardial infarction, atherosclerosis, Parkinson's disease, autoimmune diseases, radiation injury, emphysema, sunburns and cancer initiation [1]. In case of endotoxin shock these free radicals can kill the host but body has a self defense system in the form of superoxide dismutase (SOD), glutathione peroxidase (GPx), catalase, vitamins and biological dyes to neutralize the damage of free radicals. In cancer patients however these free radicals are produced in comparatively larger amounts therefore, if a compound which is aimed for the treatment of cancer has free radical scavenging activity, then its value increases.

Lower NO levels are important to protect the body organs from damage. Ischemic damage for example, is a condition in which blood supply to the tissue is restricted which causes

the shortage of the glucose levels and oxygen to disturb the metabolism. NO can also contribute to the reperfusion injury i.e. after ischemic stress high levels of NO are produced which then react with superoxide radicals to produce peroxynitrile radical. Although NO is an important signaling molecule [36] but its higher levels have been related to obesity, cancer and diabetes. It is also established that cancerous cells have higher concentrations of NO than the normal cells [37].

In this article we have combined the two functionalities i.e. ferrocene and selenoureas in a new class of compounds called ferrocene incorporated selenoureas (FIS). We have discussed the synthesis and chemical characterization (FT-IR, multinuclear NMR, and elemental analysis) of six new compounds with comparative DNA binding (with cyclic voltammetry, UV-vis spectroscopy and viscometry), antioxidant studies (DPPH scavenging activity), anti-inflammatory activities (nitrite inhibition), phase I enzyme inhibition activities (aromatase inhibition), phase II enzyme induction studies (quinone reductase induction) and cytotoxic studies against neuroblastoma (MYCN2 and SK-N-SH), liver cancer (Hepa 1c1c7) and breast cancer (MCF-7) of seventeen FIS.

2. Material and Methods

Melting points were determined in a capillary tube using Gallenkamp (U.K) electrothermal melting point apparatus. Infrared spectrum was taken on Thermoscientific NICOLET 6700 FTIR between 4000-400 cm^{-1}. ^{1}H and ^{13}C spectra were recorded between 0-13 ppm and 0-210 ppm respectively on Jeol JNM-LA 500 FT-NMR. $Si(CH_3)_4$ was used as internal reference. The elemental analysis was performed using a LECO-932 CHNS analyzer while the Fe

concentrations were determined on an Atomic Absorption Spectrophotometer Perkin Elmer 2380.

Commercial salmon DNA was solubalized in doubly distilled water to prepare a stock solution of 5.88 x 10^{-4} M from which working concentrations of DNA were prepared. Concentration of stock solution was measured by UV absorbance at 260 nm using an epsilon value of 6600 $M^{-1}cm^{-1}$. This DNA was protein free because $A_{260}/A_{280} > 1.8$. Working solutions for DNA binding studies were prepared by our previously reported method [13].

In CV studies a three electrode system was used consisting of working (platinum disc electrode with a geometric area of 0.071 cm^2) reference (Ag/AgCl) and auxiliary electrodes (platinum electrode with geometric area much greater than working electrode). Changes in peak current and peak potential provided the information about drug-DNA binding constant and mode of interaction respectively. The changes in peak current of the free drug (test compounds in absence of DNA) by the addition of varying concentrations of DNA was used to evaluate the drug-DNA binding constant with the help of following equation [38]:

$$\log (1/[DNA]) = \log K + \log (I/I_{\circ} - I) \quad \text{Eq 1}$$

Where K is the binding constant and $I_{\circ}$ and I are the peak currents of free drug and DNA bound drug respectively.

For the measurement of binding site size (s) following equation was used [39]:

$$C_b/C_f = K[(\text{free base pairs})/s] \quad \text{Eq 2}$$

Where s is the binding site size in terms of base pair, K is the binding constant, C_f is the concentration of free species and C_b represents concentration of drug-DNA bound species.

Considering the concentration of DNA in terms of nucleotide phosphate, the concentration of DNA base pair will be taken as [DNA base pair]/2 and Eq 2.4 will be written as [31]:

$C_b/C_f = K[(\text{DNA base pair})/2s]$ Eq 3

The value of C_b/C_f is equal to $(I_\circ - I/I)$ which are the values of experimental peak currents.

For the determination of diffusion coefficient of free and DNA bound drug following form of Randles-Sevcik Equation was used [32]:

$I_{pa} = 2.69 \times 10^5 \, n^{3/2} A \, C_\circ^{*} \, D_\circ^{1/2} \upsilon^{1/2}$ Eq 4

Where I_{pa} is the anodic peak current in ampere, $C_\circ^{*}$ is the reductants's concentration in $molcm^{-3}$, υ is the scan rate in $volts^{-1}$, A is the geometric area of the electrode in cm^2, n is the number of electrons involved in the process and $D_\circ$ is the diffusion coefficient in cm^2s^{-1}. Same procedure was followed for the interaction of surfactants with FIS.

Absorption spectra were recorded on Shimadzu 1800 spectrophotometer. First the spectra for the solution of pure compounds were recorded between 220-800 nm in the absence of DNA and then in the presence of different concentration of DNA. Equal amount of DNA was added to both reference and sample cells in order to avoid the appearance of its peak at 260 nm.

The Ubbelohde viscometer was used for viscosity measurements at room temperature (25 ± 1 °C). Flow time was measured with a digital stopwatch. Flow time measurements were made in triplicate for the measurement of average flow time. Data were presented as relative specific viscosity (η/η_o), vs. binding ratio ([compound]/[DNA]) where η is the viscosity of DNA in the presence of complex and η_o is the viscosity of DNA alone.

Reducing abilities of all the FIS were determined by monitoring the decrease in the absorbance (with micropipette reader or UV-vis spectrophotometer) at 517 nm of 1,1-diphenylpicrylhydrazyl radical to form 1,1-diphenylpicrylhydrazine. Scavenging activity values were calculated by following equation:

Scavenging activity (%) = A_o-A/A_o x 100 Eq 5

Where A_o is the absorbance of DPPH alone and A is the absorbance of DPPH with different FIS.

Nitrite inhibition assay was performed according to a previously reported method [33]. According to this method, inside a 96-well plate, 10 x 10^4 cells/plate of RAW 264.7 cells (murine leukemia) were seeded in 10% FBS containing DMEM (Dulbecco's Modified Eagle Medium) for 24 h. Then the media was replaced with 1% FBS-containing (190 µL) phenol red free DMEM and the cultured cells were treated with 10 µL of test samples in 10% DMSO for 15 min. Then each plate was treated with 1 µgmL^{-1} of LPS for 20 h. Quantitative estimation of nitrite (which is the major oxidation product of NO) was carried out by reacting the incubation media with Griess reagent (90 µL of 1% sulfanilamide in 5% phosphoric acid, and 90 µL of N-(1-Naphthyl)ethylenediamine). Absorbance was scanned at 540 nm according to Eq 5 for percentage inhibition values.

For aromatase inhibition activity [33], test samples of synthesized compounds were preincubated with NADPH generating system at 37 °C for 10 min. Further incubation for 30 min at 37 °C was carried out before quenching with NaOH after adding the enzyme and substrate to the plates which contained NADPH generating system. The addition of NaOH terminates the reaction and after complete termination the plates were incubated for further 2 h to improve the signal to noise ratio. Fluorescence measurement was carried out at 485 and 530 nm for triplicate readings of five different concentrations of the test samples using Letrozole as a positive control.

QR (quinone reductase) assay was carried out with hepa 1c1c7 (murine hepatoma) cells which were plated with 200 µL per well with a cell density of 0.5 x 10^4 cells/mL in MEM-α (minimum essential medium) without ribonucleosides or deoxyribonucleosides, supplemented with antimycotic/antibiotic and 10% FBS for 24 h in a carbon dioxide incubator. After 24 h medium was replaced with 190 µL of fresh medium and 10 µL of test samples were added for a final concentration of 4 ppm. After 48 h of incubation, cell membrane was permeabilized with digitonin and enzyme activity was measured by the reduction of 3-(4,5-dimethylthiazo-2-yl)-2,5-diphenyltetrazolium bromide (MTT) to a blue formazan. 4-bromoflavone was used as a positive control and production was measured by absorption at 595 nm [40] with a total protein assay using crystal violet staining run, in parallel [41]. Test samples with an induction ratio > 2 were tested in a 5 fold serial dilutions to determine the CD values [33].

The cytotoxic activities of the test compounds were carried out against neuroblastoma cell lines MYCN-2 and SK-N-SH, hepa 1c1c7 liver carcinoma cell line, human breast cancer cell line MCF-7. Briefly, 10 µL of test compounds in all the three series were filled in 96-well plate using 10% DMSO in phosphate buffered saline along with 190 µL of cells (5 x 10^4 cells/mL) and incubated at 37 °C for 72 h in a carbon dioxide incubator. After quenching the incubation with 50 µL of cold 20% trichloroacetic acid, the cells were washed, air dried and stained with 0.4% SRB in 1% acetic acid for 30 min at room temperature. Wells were then washed 4 times with 1% acetic acid solution and plates were dried for 12 h. Bound dye was solubalized in trisbase (200 µL, 10 mM, pH 10) for 10 min on gyratory shaker. For the measurement of optical density at 515 nm, microplate reader (bio-tek) was used which gave information about percent survival. Zero day control was performed in each case with all the procedure mentioned above [33].

Ferrocene, anilines, sodium nitrite, diethyl ether, acetone, DMSO, Pd-charcoal, carboxylic acid chlorides and hydrazine were purchased from Sigma Aldrich. Ferrocenyl anilines were synthesized by a procedure reported by our group previously [42].

3. Experimental

3.1 General procedure

For the synthesis of FIS, respective carboxylic acid chloride was reacted with potassium selenocyanate in 1:1 using dried acetone as a solvent inside a two necked round bottom flask under constant magnetic stirring. This resulted in the formation of white precipitates of potassium chloride with yellow isoselenocyanate in the solution. The reaction was carried out for 3 h to completion and then respective ferrocenylphenylaniline was added (1:1 with acid chloride and KSeCN) (Scheme 1). The reaction took almost 4 h for completion and the progress of reaction was monitored with the help of thin layer chromatography. The resulting orange colored solution was mixed with cold water under constant magnetic stirring. This removed the potassium chloride suspension and precipitated the product which was then filtered, dried and washed with n-hexane and methanol [1, 10-14, 43-46].

3.1.1 1-(2-methylbenzoyl)-3-(4-ferrocenylphenyl)selenourea (A-1)

Yield: 63%; **Decomposition temperature:** 130-132 °C; **FT-IR** (cm^{-1}): 3400-3200 (NH stretching broad), 3013 (Aromatic-H stretching), 2968 (Aliphatic-H), 1666 (C=O stretching), 1597, 1525, 1511 (C=C stretching of aromatic ring), 1365 (CH_3 bending) 1229 (C=Se stretching); **^{1}H-NMR** (300 MHz, Benzene, δ (ppm): 13.41 (s, 1H, CSeNH), 9.10 (s, 1H, CONH), 7.98-6.67 (m, 8H, Aromatic), 4.55 (t, 2H, *J* 1.8 Hz, Cp-Ph), 4.23 (t, 2H, *J* 1.8 Hz, Cp-Ph), 4.00 (s, 5H, Cp), 2.37 (s, 3H, CH_3); **^{13}C-NMR** (75 MHz, Benzene, δ (ppm): 178.0 (1C), 169.0 (1C),

138.5 (1C), 133.4 (1C), 126.1 (2C), 126.0 (2C), 125.5 (1C), 125.1 (1C), 123.5 (1C), 122.0 (1C), 121.7 (1C), 121.3 (1C), 84.6 (1C), 69.9 (5C), 69.7 (2C), 66.3 (2C), 19.9 (1C); **Anal.** Calcd. for $C_{25}H_{22}N_2OFeSe$: C 59.88, N 5.51, H 4.39, Fe 11.17; Found: C 59.58, N 5.29, H 3.99, Fe 10.99%.

3.1.2 1-(3-methylbenzoyl)-3-(4-ferrocenylphenyl)selenourea (A-2)

Yield: 77%; **Decomposition temperature:** 141-143 °C; **FT-IR** (cm^{-1}): 3400-3200 (NH stretching broad), 3010 (Aromatic-H stretching), 2968 (Aliphatic-H), 1664 (C=O stretching), 1592, 1527, 1490 (C=C stretching of aromatic ring), 1367 (CH_3 bending), 1231 (C=Se stretching); **^{1}H-NMR** (300 MHz, Benzene, δ (ppm): 13.08 (s, 1H, CSeNH), 10.30 (s, 1H, CONH), 7.52-6.14 (m, 8H, Aromatic), 4.55 (t, 2H, *J* 2.1 Hz, Cp-Ph), 4.23 (t, 2H, *J* 1.8 Hz, Cp-Ph), 4.21 (s, 5H, Cp), 2.29 (s, 3H, CH_3); **^{13}C-NMR** (75 MHz, Benzene, δ (ppm): 179.2 (1C), 163.6 (1C), 136.5 (1C), 134.1 (1C), 127.0 (1C) 126.9 (1C) 126.7 (2C), 126.1 (2C), 125.6 (1C), 123.9 (1C), 122.0 (1C) 114.4 (1C), 84.0 (1C), 69.8 (5C), 69.7 (2C), 66.6 (2C), 20.1 (1C); **Anal.** Calcd. for $C_{25}H_{22}N_2OFeSe$: C 59.88, N 5.51, H 4.39, Fe 11.17; Found: C 59.33, N 5.41, H 4.32, Fe 11.08%.

3.1.3 1-(4-methylbenzoyl)-3-(4-ferrocenylphenyl)selenourea (A-3)

Yield: 83%; **Decomposition temperature:** 151-153 °C; **FT-IR** (cm^{-1}): 3400-3200 (NH stretching broad), 3012 (Aromatic-H stretching), 2967 (Aliphatic-H), 1680 (C=O stretching), 1594, 1530, 1493 (C=C stretching of aromatic ring), 1365 (CH_3 bending), 1241 (C=Se stretching); **^{1}H-NMR** (300 MHz, Benzene, δ (ppm): 13.31 (s, 1H, CSeNH), 9.47 (s, 1H, CONH), 8.02-7.32 (m, 8H, Aromatic), 4.78 (t, 2H, *J* 1.8 Hz, Cp-Ph), 4.35 (t, 2H, *J* 2.1 Hz, Cp-Ph), 4.04 (s, 5H, Cp) 2.41 (s, 3H, CH_3); **^{13}C-NMR** (75 MHz, DMSO, δ (ppm): 178.1 (1C), 167.7 (1C),

136.0 (1C), 135.7 (1C), 131.1 (1C), 128.3 (2C), 125.2 (2C), 122.6 (2C), 120.9 (1C), 114.0 (2C), 84.4 (1C), 69.4 (5C), 69.3 (2C), 66.0 (2C), 20.6 (1C); **Anal.** Calcd. for $C_{25}H_{22}N_2OFeSe$: C 59.88, N 5.51, H 4.39, Fe 11.17; Found: C 59.73, N 5.43, H 4.01, Fe 11.00%.

3.1.4 1-(2-chlorobenzoyl)-3-(4-ferrocenylphenyl)selenourea (A-4)

Yield: 64%; **Decomposition temperature:** 134-136 °C; **FT-IR** (cm^{-1}): 3400-3200 (NH stretching broad), 3009 (Aromatic-H stretching), 1662 (C=O stretching), 1598, 1526, 1500 (C=C stretching of aromatic ring), 1246 (C=Se stretching); **^{1}H-NMR** (300 MHz, Acetone, δ (ppm): 12.92 (s, 1H, CSeNH), 10.01 (s, 1H, CONH), 8.01-7.15 (m, 8H, Aromatic), 4.54 (t, 2H, *J* 2.1 Hz, Cp-Ph), 4.30 (t, 2H, *J* 1.8 Hz, Cp-Ph), 4.17 (s, 5H, Cp); **^{13}C-NMR** (75 MHz, Acetone, δ (ppm): 178.0 (1C), 167.6 (1C), 136.5 (1C), 136.0 (1C), 134.1 (1C), 133.8 (1C), 133.0 (1C), 132.0 (1C), 126.9 (2C), 126.0 (2C), 123.4 (1C), 118.6 (1C), 84.5 (1C), 69.7 (5C), 69.0 (2C), 66.1 (2C); **Anal.** Calcd. for $C_{24}H_{19}N_2OFeSeCl$: C 55.25, N 5.37, H 3.64, Fe 10.70; Found: C 55.21, N 5.02, H 3.51, Fe 10.63%.

3.1.5 1-(3-chlorobenzoyl)-3-(4-ferrocenylphenyl)selenourea (A-5)

Yield: 79%; **Decomposition temperature:** 136-137 °C; **FT-IR** (cm^{-1}): 3400-3200 (NH stretching broad), 3002 (Aromatic-H stretching), 1662 (C=O stretching), 1598, 1528, 1513 (C=C stretching of aromatic ring), 1242 (C=Se stretching); **^{1}H-NMR** (300 MHz, Acetone, δ (ppm): 13.29 (s, 1H, CSeNH), 9.16 (s, 1H, CONH), 7.97-6.58 (m, 8H, Aromatic), 4.56 (t, 2H, *J* 1.8 Hz, Cp-Ph), 4.24 (t, 2H, *J* 1.5 Hz, Cp-Ph), 4.01 (s, 5H, Cp); **^{13}C-NMR** (75 MHz, Acetone, δ (ppm): 179.1 (1C), 165.1 (1C), 138.7 (1C), 134.6 (1C), 133.0 (1C) 130.1 (2C), 129.2 (1C), 126.9 (1C), 126.8 (1C), 125.1 (2C), 123.2 (1C), 120.9 (1C), 84.5 (1C), 69.2 (5C), 68.8 (2C), 66.7 (2C); **Anal.**

Calcd. for $C_{24}H_{19}N_2OFeSeCl$: C 55.25, N 5.37, H 3.64, Fe 10.70; Found: C 54.89, N 5.19, H 3.55, Fe 10.54%.

3.1.6 1-(4-chlorobenzoyl)-3-(4-ferrocenylphenyl)selenourea (A-6)

Yield: 81%; **Decomposition temperature:** 159-160 °C; **FT-IR** (cm^{-1}): 3400-3200 (NH stretching broad), 3021 (Aromatic-H stretching), 1678 (C=O stretching), 1598, 1540, 1505 (C=C stretching of aromatic ring), 1268 (C=Se stretching); **^{1}H-NMR** (300 MHz, Acetone, δ (ppm): 12.89 (s, 1H, CSeNH), 11.94 (s, 1H, CONH), 8.05-7.52 (m, 8H, Aromatic), 4.75 (t, 2H, *J* 1.8 Hz, Cp-Ph), 4.33 (t, 2H, *J* 1.8 Hz, Cp-Ph), 4.02 (s, 5H, Cp); **^{13}C-NMR** (75 MHz, Acetone, δ (ppm): 178.4 (1C), 169.0 (1C), 136.4 (1C), 136.0 (1C), 131.4 (1C) 130.7 (2C), 129.3 (2C), 126.3 (2C), 126.0 (2C), 125.8 (1C), 84.3 (1C), 69.3 (5C), 69.2 (2C), 69.0 (2C); **Anal.** Calcd. for $C_{24}H_{19}N_2OFeSeCl$: C 55.25, N 5.37, H 3.64, Fe 10.70; Found: C 54.88, N 5.29, H 3.39, Fe 10.41%.

4. Results and Discussion

All the compounds are orange in color and were synthesized in solid state. In ^{1}H NMR spectra (Figure S-1) there are three different types of protons i.e. –NH protons, aromatic protons and protons of the ferrocene ring in all the compounds. Maximum downfield protons are the ones which are between the phenyl ring and C=Se groups and provides a singlet at ~ 13 ppm in all the compounds because of the intramolecular hydrogen bonding. The protons between the carbonyl and C=Se in all the compounds are comparatively less deshielded and appears at ~ 10 ppm as a singlet. Aromatic protons are available between 7-8 ppm whereas five protons of unsubstituted cylopentadienyl (Cp) moiety give a singlet at 4.11 ppm for both the compounds. Substituted Cp ring provides two triplets with a coupling constant value of 1.8 Hz downfield from the singlet of

unsubstituted Cp in all the compounds [1, 10-14, 43-46]. In ^{13}C NMR (Figure S-2) maximum downfield carbon is the carbon attached with selenium and appears as a weak signal at ~ 179 ppm whereas carbonyl carbon is available at ~ 162 ppm. Aromatic carbons give their peaks between 120-140 ppm and unsubstituted Cp gives a singlet at ~ 66 ppm. In all the compounds substituted carbon of the Cp ring gives a peak at ~ 84 ppm whereas four other carbons of the substituted Cp ring give two peaks at ~ 69 ppm [1, 10-14, 43-46].

In FT-IR all the compounds provide broad peaks between 3200-3400 cm^{-1} owing to the intramolecular hydrogen bonding. Aromatic-H provide their signals slightly above 3000 cm^{-1} whereas carbonyl carbons are available at ~ 1660 cm^{-1} for all the compounds. Aromatic rings yield their peak in their respective region and C=Se is present at ~ 1200 cm^{-1} for all the compounds [1, 10-14, 43-46].

Calculated and found percentages of carbon, hydrogen, nitrogen and iron are in close agreement with each other which confirms the purity of the synthesized compounds. We have already published the single crystal XRD structures of a few FIS (Figure 1) in our previous publications [12, 13] but details cancer studies are the main concern in this manuscript.

4.1 Carcinogenesis

4.1.1 DNA binding studies

In CV all the synthesized FIS provide couple of well defined redox peaks between 0-1V in a 100% reversible electrochemical process (Figure 2a) by using 1mL of 1.5 M KCl as supporting electrolyte.

The reversibility of the process was evident by:

- Absence of a shift in peak potentials with a variation in scan rate.
- $\Delta E_p = E_{pc} - E_{pa}$ for one electron system gives a value of almost 59 mV.
- Anodic and cathodic peak current ratios (I_{pa}/I_{pc}) of about one [13].

DNA binding study of a representative compound A-3 is explained here with CV. In CV A-3 provides couple of well defined redox peaks which show 100% reversibility according to the criteria described above (Figure 2a). By the addition of DNA to the free A-1 (by keeping the dilution constant) there is a negative shift in the peak potential of A-3-2 μMDNA adduct relative to the free A-3 (Figure 2b). This negative shift in the peak potential represents the electrostatic mode of interaction between the negatively charged phosphate backbone of the DNA and A-3 which makes the oxidation of A-3 easy. Decrease in the current is attributed to the slow diffusion of A-3-DNA adducts relative to free A-3 which was also confirmed by the low diffusion coefficient of adducts relative to the free A-3 (Figure 2c). This uniform decrease in the current with different DNA concentrations was scanned for the determination of A-3-DNA binding constant according to the Eq. 1 above (Figure 2d). Lower values of the binding site (Eq. 2) also confirm the electrostatic mode of interaction (Figure 2e). Similar type of electrostatic interaction was confirmed by hyperchromism in the absorbance of DNA solution by the addition of different concentrations of A-3 to it in UV-vis spectroscopy. Same amounts of A-3 were also added in the blanks to avoid its absorbance in the same region. This hyperchromism is attributed to the neutralization of charges on the phosphate backbone of the DNA which causes the unwinding of DNA double helix to cause the conformational changes (Figure 3a). Moreover decrease in the relative viscosity of the DNA also confirms the electrostatic mode of interaction (Figure 3b) [1, 10-14]. Data for all other compounds have been presented in Table 1 which reveals that, para substituted derivatives generally show higher DNA binding constants than that of meta and ortho

substituted derivatives. Diffusion coefficients of drug-DNA adducts for all the compounds are lower than the free drugs and lower values of binding site sizes are also in favor of electrostatic interactions. Magnitude of DNA binding constants reported in this paper are better than ferrocene [31], nitrophenyl ferrocene [32], ferrocene incorporated thioureas [47], cis-platin [48] and most of the closely related platinum, copper, nickel and zinc complexes [49] but are inferior than the universal intercalators like ethidium [50] and proflavin [51]. These DNA binding studies provided us very good preliminary information about possible chemopreventive nature of FIS.

4.1.2 DPPH scavenging activity

Here we present the results for DPPH scavenging activities by synthesized FIS, using ascorbic acid as a positive control. Figure 4 displays the results for antioxidant effects of FIS to convert the DPPH to 1,1-diphenylpicryl hydrazine. Generally, the compounds which have electron withdrawing groups attached to them are more active than those which have electron donating groups because the free radical formed are more stabilized by the electron withdrawing groups. This uniform behavior originates because of the antioxidant effect of the –NH groups present in the structures of the synthesized FIS, however there are two –NH groups and both of them compete with each other to cause the discrepancies in the structure and activity relationship (Chart 2). Discrepancy in case of 4-methylphenyl and 2-methylphenyl derivatives may be because of the special role played by the Se atom. FIS which show more than 50% inhibition of DPPH were scanned for IC_{50} values (Figure 5a) with the help of UV-vis spectroscopy (Figure 5b).

4.1.3 Nitrite inhibition activity

Raw 264.7 (tumor tissue of male mouse with murine leukemia) cells were used to determine the NO inhibition of synthesized FIS using LNMMA (L-N-monomethyl arginine citrate) as a positive control. Figure 6 shows the NO inhibition activity of the synthesized FIS which is even better than the positive control for more than 10 compounds. The compounds which presented more than 50% inhibition were scanned for IC_{50} values as well (Figure 7a). Although a generalization cannot be developed on the basis of structure but higher activity of ortho substituted derivatives (2-fluorophenyl, 2-chlorophenyl, 2-bromophenyl and 2-methoxyphenyl) may be due to the formation of more active byproduct presented in Figure 7b. Whereas higher activity of toulyl substituted derivatives may be because of their higher permeability through the cell membrane but conformation to this hypothesis needs more detail study by the biochemists and biotechnologists.

4.1.4 Enzymatic activities

In terms of carcinogenesis, those compounds are good anticancer agents who can inhibit phase I enzymes (cytochrome P_{450}) and induce the phase II enzymes (glutathione S-transferases (GSTs), UDP-glucuronosyl transferases, and quinone reductases). The reason behind is that phase I enzymes favor the production of reactive oxygen species (ROS) which are initiator of the cancers whereas phase II enzymes detoxify the ROS and effects caused by them to stop the propagation of the cancer. Phase I (aromatase inhibition) and phase II (quinone reductase induction) activities of the synthesized FIS have been presented below to have the glimpse about their chemopreventive nature.

4.1.4.1 Aromatase inhibition activity

Aromatase is the enzyme which controls a key step in the biosynthesis of estrogen. Lower concentrations of estrogen are required to fight the breast cancer, ovarian cancer and lungs

cancer. Recent investigations have shown that aromatase inhibitors are even better than the tamoxifen for the treatment of breast cancer [52].

Figure 8a puts on show the aromatase inhibition activities of the synthesized FIS. Although the synthesized FIS inhibit aromatase but their activity is inferior to the positive control however some activities are better than cis-platin. The best activity in this regard was presented by the precursor aniline (paraferrocenylphenylaniline) which shows 100% inhibition of aromatase (even more than the positive control). The compounds which show more than 50% inhibition of aromatase have been evaluated for IC_{50} values (Figure 8b).

4.1.4.2 Quinone reductase induction activity

Quinone reductase induction activity was carried out inside hepa 1c1c7 (murine hepatoma) cells. For this activity induction ration of QR1 (IR of QR1) are the values which represent the specific enzyme activity of agent treated cells compared with a DMSO treated control. And the compounds which have an induction ratio of more than 2 are further evaluated for concentration dose (CD) experimentation. CD is the concentration of a chemical under investigation which doubles the QR activity. Figure 9 presents the results of QR induction for the synthesized compounds and it is evident from the results that most the compounds have an induction ratio of greater than 2 which makes them a very good candidate for CD experimentation.

CD (μM) (Figure 10) values reveal that most of the compounds have better activities than previously reported unsymmetrical diphenyl selenourea and all of them are better than unsymmetrical dimethyl selenourea [1] (Chart 3). Both the aromatase inhibition and quinone reductase induction activities prove that the synthesized FIS have the ability to stop the cancer initiation and cancer propagation [53]. In terms of enzymology these compounds are even better

than cis-platin, in a way that cis-platin only kills the cancerous cells by covalent binding with DNA (because of its cytotoxic effect) and does not have any importance to stop the initiation of the cancer or to equip the body with the enzymes which can themselves fight the cancer.

4.1.5 Activities against the cancer cell lines

Cytotoxic activities have been carried out against four cancerous cell lines namely neuroblastoma cell lines (MYCN2 and SK-N-SH), lungs cancer cell line (hepa 1c1c7) and breast cancer cell line MCF-7 to further investigate the chemopreventive nature of the synthesized FIS.

4.4.5.1 Neuroblastoma

Neuroblastoma is a type of malignant extracranial cancer of the childhood between the age of 1-5 years [54]. There are 650 cases/year in USA and 100 cases/year in UK. This cancer is caused by the over expression of a protein called NMYc which is controlled by a gene called MYCN (neuroblastoma myelocytomatosis). This protein has an important function in the transfer of the genetic information by binding with the DNA. It is believed that if over expression of NMYc is controlled by inhibiting MYCN then neuroblastoma will be controlled [55]. Table 2 displays the data for the compounds scanned against MYCN. The data very clearly presents that synthesized FIS can kill up to 70-90% of cancerous cells. Although few exceptions are there but mostly ortho substituted derivatives have shown the highest activities.

Another neuroblastoma cell line SK-N-SH was also scanned for cytotoxic activities with the help of the synthesized FIS but data for only the most active compounds have been presented in Table 2. The activity against this cell lines is comparatively too much inferior than MYCN2.

4.4.5.2 Cytotoxicity against hepa 1c1c7 and liver cancer

Liver cancer is the 5th most diagnosed cancer of the world and is mostly caused by hepatitis B and hepatitis C. The synthesized FIS have shown 27-37% cell killings against this cancer cell line hepa1c1c7. Table 2 presents data for the most active FIS.

4.4.5.3 Cytotoxicity against MCF-7 and breast cancer

Breast cancer is 22.7% of all the cancers in the world and in 2008 13.7% of cancer deaths were caused because of this cancer. It is 100 time more common in females than in males [56]. Table 2 presents the data for the synthesized FIS against breast cancerous cell line MCF-7. Ortho substituted derivatives once again have shown the highest activities as was observed against neuroblastoma.

Conclusions

We have successfully reported the chemopreventive nature of ferrocene incorporated selenoureas (FIS) against cancer initiation, cancer propagation and cancer termination. We found that FIS are good DPPH scavengers in comparison with ascorbic acid although their IC_{50} values are slightly inferior. Anti-inflammatory action of some FIS is even better than the positive control (L-NMMA). FIS reported in this article can inhibit aromatase (phase I enzyme) and can induce the quinone reductase (phase II enzyme) in the body and these two enzymatic potencies are even better than cis-platin. Cancer termination of the FIS is proved by their cytotoxic activities against neuroblastoma, hepa 1c1c7 and MCF-7 cancerous cell lines. Mostly those FIS which had ortho substitution on the phenyl ring attached with the carbonyl carbon were found the most active.

Corresponding Author

Prof. Amin Badshah: aminbadshah@yahoo.com, +923009780374.

Acknowledgements

I am thankful to the Higher Education Commission, H-9, Islamabad, Pakistan for research funding.

References

[1] R.A. Hussain, A. Badshah, A. Shah, Synthesis and biological applications of selenoureas, Appl. Organomet. Chem., 28 (2014) 61-73.

[2] H. Takahashi, A. Nishina, R.-h. Fukumoto, H. Kimura, M. Koketsu, H. Ishihara, Selenocarbamates are effective superoxide anion scavengers in vitro, Eur. J. Pharm. Sci., 24 (2005) 291-295.

[3] H. Takahashi, A. Nishina, R.-h. Fukumoto, H. Kimura, M. Koketsu, H. Ishihara, Selenoureas and thioureas are effective superoxide radical scavengers in vitro, Life Sci., 76 (2005) 2185-2192.

[4] H. Takahashi, A. Nishina, H. Kimura, K. Motoki, M. Koketsu, H. Ishihara, Tertiary selenoamide compounds are useful superoxide radical scavengers in vitro, Eur. J. Pharm. Sci., 23 (2004) 207-211.

[5] H. Tsukagoshi, M. Koketsu, M. Kato, M. Kurabayashi, A. Nishina, H. Kimura, Superoxide radical-scavenging effects from polymorphonuclear leukocytes and toxicity in human cell lines of newly synthesized organic selenium compounds, FEBS J., 274 (2007) 6046-6054.

[6] M. Ishiyama, Y. Miyazono, K. Sasamoto, Y. Ohkura, K. Ueno, A highly water-soluble disulfonated tetrazolium salt as a chromogenic indicator for NADH as well as cell viability, Talanta, 44 (1997) 1299-1305.

[7] K. Sivapriya, P. Suguna, A. Banerjee, V. Saravanan, D.N. Rao, S. Chandrasekaran, Facile one-pot synthesis of thio and selenourea derivatives: A new class of potent urease inhibitors, Bioorg. Med. Chem. Lett., 17 (2007) 6387-6391.

[8] G. Roy, D. Das, G. Mugesh, Bioinorganic chemistry aspects of the inhibition of thyroid hormone biosynthesis by anti-hyperthyroid drugs, Inorg. Chim. Acta, 360 (2007) 303-316.

[9] D. Desai, S.V. Madhunapantula, K. Gowdahalli, A. Sharma, R. Chandagaludoreswamy, K. El-Bayoumy, G.P. Robertson, S. Amin, Synthesis and characterization of a novel iNOS/Akt inhibitor Se,Se′-1,4-phenylenebis(1,2-ethanediyl)bisisoselenourea (PBISe)—against colon cancer, Bioorg. Med. Chem. Lett., 20 (2010) 2038-2043.

[10] R.A. Hussain, A. Badshah, K. Akbar, Comparative DNA binding and antioxidant studies of acetyl and benzoyl substituted ferrocene incorporated selenoureas, Russ. J. Electrochem., 51 (3)198-208 (2014).

[11] R.A. Hussain, A. Badshah, M. Sohail, B. Lal, K. Akbar, Synthesis, chemical characterization, DNA binding and antioxidant studies of ferrocene incorporated selenoure, J. Mol. Struct., 1048 (2013) 367-374.

[12] R.A. Hussain, A. Badshah, M.N. Tahir, T.U. Hassan, A. Bano, Synthesis, Chemical Characterization, DNA Binding, Antioxidant, Antibacterial, and Antifungal Activities of Ferrocence Incorporated Selenoureas, J. Biochem. Mol. Toxicol., 28 (2014) 60-68.

[13] R.A. Hussain, A. Badshah, M.N. Tahir, B. Lal, I.A. Khan, Synthesis, chemical characterisation, and DNA binding studies of ferrocene-incorporated selenoureas, Aust. J. Chem., 66 (2013) 626-634.

[14] R.A. Hussain, A. Badshash, M. Sohail, B. Lal, A.A. Altaf, Synthesis, chemical characterization, DNA interaction and antioxidant studies of ortho, meta and para fluoro substituted ferrocene incorporated selenoureas, Inorg. Chim. Acta, 402 (2013) 133-139.

[15] G. Mugesh, W.-W. du Mont, H. Sies, Chemistry of biologically important synthetic organoselenium compounds, Chem. Rev., 101 (2001) 2125-2180.

[16] I.B. Douglass, Acylselenoureas, J. Am. Chem. Soc., 59 (1937) 740-742.

[17] J.R. Andreesen, L.G. Ljungdahl, Formate dehydrogenase of Clostridium thermoaceticum: incorporation of selenium-75, and the effects of selenite, molybdate, and tungstate on the enzyme, J. Bacteriol., 116 (1973) 867-873.

[18] C. Ornelas, Application of ferrocene and its derivatives in cancer research, New J. Chem., 35 (2011) 1973-1985.

[19] V.J. Fiorina, R.J. Dubois, S. Brynes, Ferrocenyl polyamines as agents for the chemoimmunotherapy of cancer, J. Med. Chem., 21 (1978) 393-395.

[20] Á. Mooney, A.J. Corry, C.N. Ruairc, T. Mahgoub, D. O'Sullivan, N. O'Donovan, J. Crown, S. Varughese, S.M. Draper, D.K. Rai, Synthesis, characterisation and biological evaluation of N-(ferrocenyl) naphthoyl amino acid esters as anticancer agents, Dalton Trans., 39 (2010) 8228-8239.

[21] B. Long, S. Liang, D. Xin, Y. Yang, J. Xiang, Synthesis, characterization and in vitro antiproliferative activities of new 13-< i> cis</i>-retinoyl ferrocene derivatives, Eur. J. Med. Chem., 44 (2009) 2572-2576.

[22] L.V. Snegur, Y.S. Nekrasov, N.S. Sergeeva, Z.V. Zhilina, V.V. Gumenyuk, Z.A. Starikova, A.A. Simenel, N.B. Morozova, I.K. Sviridova, V.N. Babin, Ferrocenylalkyl azoles: bioactivity, synthesis, structure, Appl. Organomet. Chem., 22 (2008) 139-147.

[23] S. Knauer, B. Biersack, M. Zoldakova, K. Effenberger, W. Milius, R. Schobert, Melanoma-specific ferrocene esters of the fungal cytotoxin illudin M, Anti-Cancer Drugs, 20 (2009) 676-681.

[24] S. Top, B. Dauer, J. Vaissermann, G. Jaouen, Facile route to ferrocifen, 1-[4-(2-dimethylaminoethoxy)]-1-(phenyl-2-ferrocenyl-but-1-ene), first organometallic analogue of tamoxifen, by the McMurry reaction, J. Organomet. Chem., 541 (1997) 355-361.

[25] S. Top, J. Tang, A. Vessières, D. Carrez, C. Provot, G. Jaouen, Ferrocenyl hydroxytamoxifen: a prototype for a new range of oestradiol receptor site-directed cytotoxics, Chem. Commun., (1996) 955-956.

[26] S. Top, C. Thibaudeau, A. Vessieres, E. Brulé, F. Le Bideau, J.-M. Joerger, M.-A. Plamont, S. Samreth, A. Edgar, J. Marrot, Synthesis and structure activity relationship of organometallic steroidal androgen derivatives, Organometallics, 28 (2009) 1414-1424.

[27] S. Top, A. Vessières, G. Leclercq, J. Quivy, J. Tang, J. Vaissermann, M. Huché, G. Jaouen, Synthesis, Biochemical Properties and Molecular Modelling Studies of Organometallic Specific Estrogen Receptor Modulators (SERMs), the Ferrocifens and Hydroxyferrocifens: Evidence for an Antiproliferative Effect of Hydroxyferrocifens on both Hormone-Dependent and Hormone-Independent Breast Cancer Cell Lines, Chem. Eur. J., 9 (2003) 5223-5236.

[28] E.A. Hillard, A. Vessières, G. Jaouen, Ferrocene functionalized endocrine modulators as anticancer agents, in: Med. Organomet. Chem., Springer, 2010, pp. 81-117.

[29] O. Payen, S. Top, A. Vessières, E. Brulé, M.-A. Plamont, M. J. McGlinchey, H. Müller-Bunz, G. Jaouen, Synthesis and Structure–Activity Relationships of the First Ferrocenyl-Aryl-Hydantoin Derivatives of the Nonsteroidal Antiandrogen Nilutamide, J. Med. Chem., 51 (2008) 1791-1799.

[30] A.P. Ferreira, J.L.F. da Silva, M.T. Duarte, M.F.M. Da Piedade, M.P. Robalo, S.G. Harjivan, C. Marzano, V. Gandin, M.M. Marques, Synthesis and characterization of new organometallic benzo [b] thiophene derivatives with potential antitumor properties, Organometallics, 28 (2009) 5412-5423.

[31] A. Shah, R. Qureshi, N.K. Janjua, S. Haque, S. Ahmad, Electrochemical and Spectroscopic Investigations of Protonated Ferrocene-DNA Intercalation, Anal. Sci., 24 (2008) 1437-1441.

[32] A. Shah, M. Zaheer, R. Qureshi, Z. Akhter, M. Faizan Nazar, Voltammetric and spectroscopic investigations of 4-nitrophenylferrocene interacting with DNA, Spectrochem. Acta, 75 (2010) 1082-1087.

[33] I.-u.-. Haq, B. Mirza, T.P. Kondratyuk, E.-J. Park, B.E. Burns, L.E. Marler, J.M. Pezzuto, Preliminary evaluation for cancer chemopreventive and cytotoxic potential of naturally growing ethnobotanically selected plants of Pakistan, Pharm. Biol., 51 (2013) 316-328.

[34] M. Sirajuddin, S. Ali, A. Badshah, Drug–DNA interactions and their study by UV–Visible, fluorescence spectroscopies and cyclic voltametry, J. Photochem. Photobiol., B, 124 (2013) 1-19.

[35] M. Sirajuddin, S. Ali, N.A. Shah, M.R. Khan, M.N. Tahir, Synthesis, characterization, biological screenings and interaction with calf thymus DNA of a novel azomethine 3-((3,5-dimethylphenylimino)methyl)benzene-1,2-diol, Spectrochem. Acta, 94 (2012) 134-142.

[36] J. Torreilles, Nitric oxide: one of the more conserved and widespread signaling molecules, Front. Biosci. , 6 (2001) D1161-1172.

[37] F. Aktan, iNOS-mediated nitric oxide production and its regulation, Life sci., 75 (2004) 639-653.

[38] Q. Feng, N.-Q. Li, Y.-Y. Jiang, Electrochemical studies of porphyrin interacting with DNA and determination of DNA, Anal. Chim. Acta, 344 (1997) 97-104.

[39] M. Aslanoglu, G. Ayne, Voltammetric studies of the interaction of quinacrine with DNA, Anal. Bioanal. Chem., 380 (2004) 658-663.

[40] L.L. Song, J.W. Kosmeder, S.K. Lee, C. Gerhäuser, D. Lantvit, R.C. Moon, R.M. Moriarty, J.M. Pezzuto, Cancer chemopreventive activity mediated by 4′-bromoflavone, a potent inducer of phase II detoxification enzymes, Cancer Res., 59 (1999) 578-585.

[41] B.-N. Su, J.-Q. Gu, Y.-H. Kang, E.-J. Park, J.M. Pezzuto, A.D. Kinghorn, Induction of the phase II enzyme, quinone reductase, by withanolides and norwithanolides from solanaceous species, Mini-Rev. Org. Chem., 1 (2004) 115-123.

[42] S. Ali, A. Badshah, A.A. Ataf, B. Lal, K.M. Khan, Synthesis of 3-ferrocenylaniline: DNA interaction, antibacterial, and antifungal activity, Med. Chem. Res., 22 (2013) 3154-3159.

[43] R.A. Hussain, A. Badshah, N. Haider, M.D. Khan, B. Lal, Effect of surfactants on the morphology of FeSe films fabricated from a single source precursor by aerosol assisted chemical vapor deposition, J. Chem. Sci., (Firat online 2015).

[44] R.A. Hussain, A. Badshah, S. Marwat, F. Yasmin, M.N. Tahir, Iron selenide nanoparticles coated on carbon nanotubes from single source ferrocene incorporated selenourea precursor for fuel cell and photocatalytic applications, J. Organomet. Chem., 769 (2014) 58-63.

[45] R.A. Hussain, A. Badshah, F. Yasmin, M.D. Khan, M.N. Tahir, Aerosol assisted chemical vapor deposition for iron selenide thin films from single source ferrocene incorporated selenourea precursor in the presence of surfactants, Aust. J. Chem., online (http://dx.doi.org/10.1071/CH14088) (2014).

[46] R.A. Hussain, A. Badshah, A. Younis, M.D. Khan, J. Akhtar, Iron selenide films by aerosol assisted chemical vapor deposition from single source organometallic precursor in the presence of surfactants, Thin Solid Films, 567 (2014) 58-63.

[47] B. Lal, A. Badshah, A.A. Altaf, M.N. Tahir, S. Ullah, F. Huq, Synthesis, characterization and antitumor activity of new ferrocene incorporated N, N′-disubstituted thioureas, Dalton Trans., 41 (2012) 14643-14650.

[48] H. Xiao, K.L. Parkin, Induction of Phase II Enzyme Activity by Various Selenium Compounds, Nutr. Cancer, 55 (2006) 210-223.

[49] G. Barone, A. Terenzi, A. Lauria, A.M. Almerico, J.M. Leal, N. Busto, B. García, DNA-binding of nickel (II), copper (II) and zinc (II) complexes: Structure–affinity relationships, Coord. Chem. Rev., 257 (2013) 2848-2862.

[50] M. Waring, Complex formation between ethidium bromide and nucleic acids, J. Mol. Biol. , 13 (1965) 269-282.

[51] N. Shahabadi, S. Kashanian, M. Mahdavi, N. Sourinejad, DNA interaction and DNA cleavage studies of a new platinum (II) complex containing aliphatic and aromatic dinitrogen ligands, Bioinorg. Chem. Appl. , 2011 (2011).

[52] R. Schneider, A. Barakat, J. Pippen, C. Osborne, Aromatase inhibitors in the treatment of breast cancer in post-menopausal female patients: an update, Breast Cancer: Targets and Therapy, 3 (2011) 113.

[53] M. Cuendet, C.P. Oteham, R.C. Moon, J.M. Pezzuto, Quinone Reductase Induction as a Biomarker for Cancer Chemoprevention⊥, J. Nat. Prod., 69 (2006) 460-463.

[54] A.E. Evans, G.J. D'Angio, J. Randolph, A proposed staging for children with neuroblastoma. Children's cancer study group A, Cancer, 27 (1971) 374-378.

[55] G.M. Brodeur, J. Pritchard, F. Berthold, N. Carlsen, V. Castel, R. Castelberry, B. De Bernardi, A.E. Evans, M.a. Favrot, F. Hedborg, Revisions of the international criteria for neuroblastoma diagnosis, staging, and response to treatment, J. Clin. Oncol., 11 (1993) 1466-1477.

[56] S.H. Giordano, A review of the diagnosis and management of male breast cancer, The Oncologist, 10 (2005) 471-479.

Scheme 1. Synthesis of ferrocene incorporated selenoureas having 4-ferrocenylphenylaniline.

Chart 1. Compounds 1-10.

Chart 2 Different possibilities of DPPH scavenging by ferrocene incorporated selenoureas

Chart 3. CD values of previously reported selenoureas.

Figure 1. Single crystal XRD structures of a) 1-(4-methoxybenzoyl)-3-(4-ferrocenylphenyl)selenourea, b) 1-(2-fluorobenzoyl)-3-(4-ferrocenylphenyl)selenourea, c) 1-(3-fluorobenzoyl)-3-(4-ferrocenylphenyl)selenourea, d) 1-(2-bromobenzoyl)-3-(4-ferrocenylphenyl)selenourea.

Figure 2. a) Cyclic voltammograms of 1 mM A-1 with 1 mL of 1.5 M KCl as a supporting electrolyte at different scan rates. b) Cyclic voltammograms of 1 mM A-1 with different DNA concentrations. c) Plots of I vs. $\upsilon^{1/2}$, for the determination of diffusion coefficients of A-1 (0 µM DNA) and 2 µM DNA bound A-1. d) Plot of log ($I/I_{\circ}$-I) vs. log (1/[DNA]) for determination of binding constant. e) Plot of C_b/C_f vs. [DNA] (µM) for determination of binding site size of 2-8 µM DNA concentrations.

Figure 3. a) Plot of absorbance vs. wavelength of pure DNA and different DNA-A-1 adducts. b) Effect of increasing concentrations of A-1 on relative specific viscosity at 25 ± 1 °C.

Figure 4. %age DPPH scavenging by FIS using ascorbic acid as a positive control. General structure for the compounds is presented within the figure whereas different R groups provide different compounds in the series.

Figure 5. a) IC_{50} values of selected FIS. b) UV-vis spectra showing decrease in the absorbance of DPPH by the addition of FIS with the structure presented in the figure.

Figure 6. %age NO scavenging by synthesized FIS using LNMMA as a positive control. General structure for the compounds has been given at the top whereas R groups are embedded within the figure.

Figure 7. a) IC_{50} values of synthesized compounds using LNMMA as a positive control for NO scavenging. b) Possible byproduct formed by the interaction of ortho substituted derivatives with NO.

Figure 8. a) Aromatase inhibition activities of FIS using letrozole as a positive control. General structureof the compounds has been given above the figure whereas R groups are embedded within the figure. b) IC_{50} values for aromatase inhibition of synthesized FIS.

Figure 9. Quinone reductase induction activities of synthesized FIS. General structure of the compounds is presented above the figure whereas R groups are embedded within the figure.

Figure 10. Concentration dose (CD) values of synthesized FIS. General structure of the compounds has been given above the figure whereas R groups are embedded within the figure.

Table 1. DNA binding parameters of the compounds determined with cyclic voltammetry. At the top is the general structure and different R groups have been mentioned within the table for different compounds.

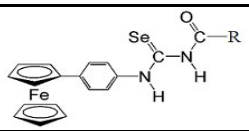

Compounds (R)	K (M^{-1})	D_o ($cm^2 s^{-1}$) Free Drug	D_o ($cm^2 s^{-1}$) Drug-DNA	s (bp)
Methyl	$4.5\ 1x\ 10^{4}$	9.14×10^{-5}	2.1×10^{-6}	1.45
Phenyl	7.69×10^{4}	5.41×10^{-5}	4.57×10^{-5}	0.83
4-fluorophenyl	4.95×10^{4}	3.44×10^{-6}	1.63×10^{-6}	0.55
3-fluorophenyl	4.70×10^{4}	4.13×10^{-6}	3.90×10^{-6}	0.46
2-fluorophenyl	7.42×10^{3}	3.54×10^{-6}	1.18×10^{-6}	1.15
4-methoxyphenyl	4.90×10^{4}	4.15×10^{-6}	3.40×10^{-6}	0.1
3-methoxyphenyl	1.29×10^{4}	6.15×10^{-7}	3.12×10^{-7}	0.27
2-methoxyphenyl	2.31×10^{4}	9.24×10^{-6}	1.36×10^{-7}	0.71
4-methylphenyl	7.43×10^{4}	9.58×10^{-7}	5.44×10^{-7}	-
3-methylphenyl	9.90×10^{3}	8.54×10^{-6}	1.38×10^{-7}	-
3-bromophenyl	$1.38x\ 10^{3}$	1.54×10^{-6}	7.4×10^{-7}	0.70
4-bromophenyl	4.39×10^{4}	3.28×10^{-6}	8.29×10^{-7}	0.20
2-bromophenyl	1.19×10^{3}	5.03×10^{-6}	3.93×10^{-6}	0.10
2-chlorophenyl	$8.30\ x10^{4}$	1.06×10^{-7}	$7.28\ x10^{-8}$	-

3-chlorophenyl	1.10×10^{3}	5.24×10^{-6}	1.06×10^{-6}	0.01

Table 2. Cytotoxicity against different cancerous cell lines of the synthesized FIS.

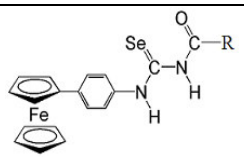 Compound (R)	MYCN-2		SK-N-SH		Hepa 1c1c7		MCF-7	
	% Survival	SD (±)	% Survival	SD (±)	% Survival	SD (±)	% Survival	SD (±)
Methyl	42.3	3.9	86.7	9.3	77.9	0.5	47.6	1.5
Phenyl	37.3	6.1	93.8	0.6	92.3	1.2	67.0	3.5
2-fluorophenyl	**26.5**	**0.6**	67.8	10.0	-		**27.0**	**0.6**
3-fluorophenyl	54.9	1.5	96.0	0.8	-		70.3	3.2
4-fluorophenyl	75.3	9.3	99.1	0.1	98.1	1.6	80.7	9.3
3-chlorophenyl	91.9	5.8	99.1	0.3	93.4	4.3	74.2	2.4
4-chlorophenyl	82.2	9.2	97.2	0.6	-		70.7	10.2
2-bromophenyl	**12.2**	**3.1**	65.6	0.6	71.5	1.3	-	
3-bromophenyl	76.4	9.3	113.1	18.1	-		75.4	9.0
2-methoxyphenyl	**18.9**	**1.0**	96.8	1.3	66.9	2.7	85.2	14.5
3-methoxyphenyl	79.9	9.3	99.1	0.2	-		-	
4-methoxyphenyl	69.3	9.6	-		-		-	
2-methylphenyl	**38.9**	**9.8**	69.1	14.3	96.0	2.7	-	
3-methylphenyl	35.7	7.8	89.8	2.5	-		85.3	19.4
4-methylphenyl	38.8	8.3	98.2	0.2	93.0	2.7	54.5	0.5
Aniline	27.3	2.4	70.0	6.8	63.1	1.3	90	6.9

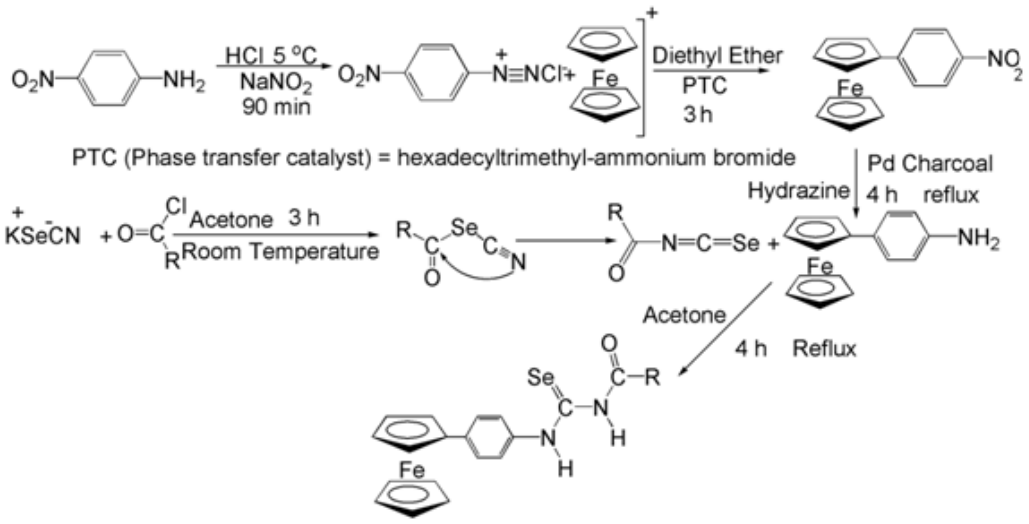

Where R = methyl, phenyl, 2-fluorophenyl, 3-fluorophenyl, 4-fluorophenyl, 2-bromophenyl, 3-bromophenyl, 4-bromophenyl, 2-chlorophenyl, 3-chlorophenyl, 4-chlorophenyl, 2-methylphenyl, 3-methylphenyl, 4-methylphenyl, 2-methoxyphenyl, 3-methoxyphenyl, 4-methoxyphenyl

Scheme 1. Synthesis of ferrocene incorporated selenoureas having 4-ferrocenylphenylaniline.

Chart 1. Compounds 1-10.

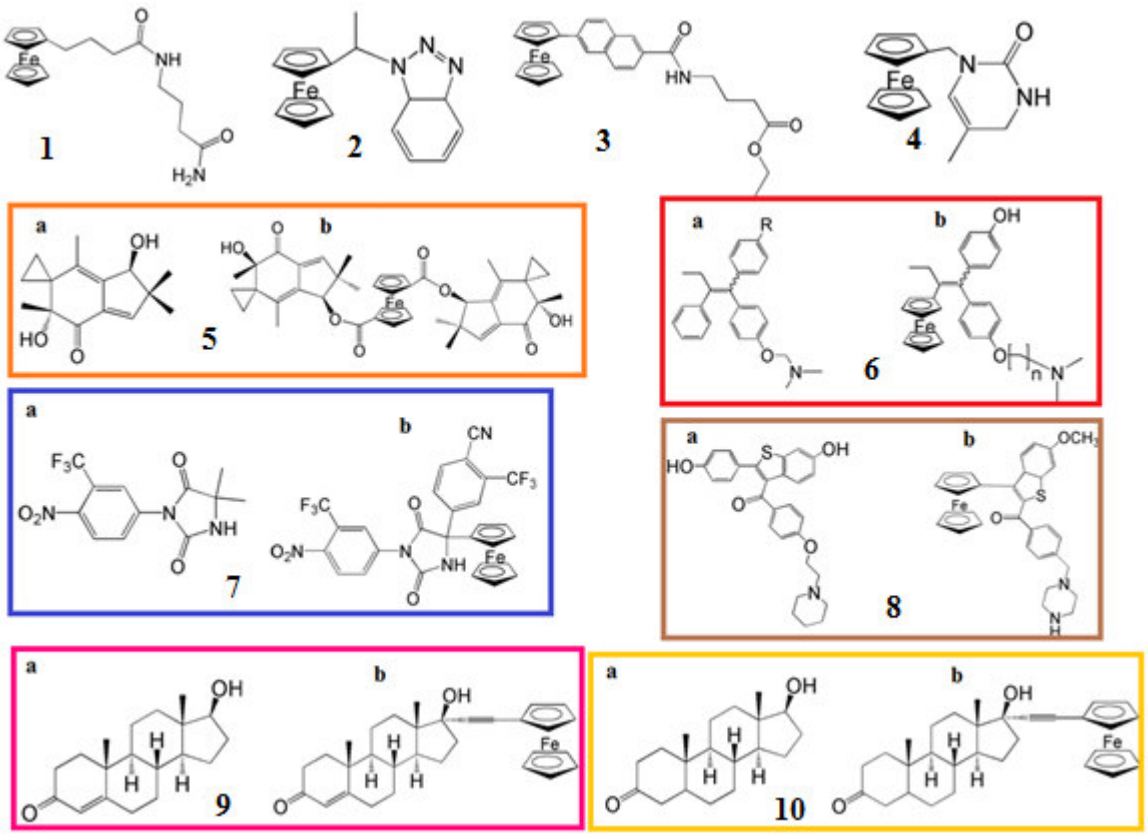

Chart 2 Different possibilities of DPPH scavenging by ferrocene incorporated selenoureas

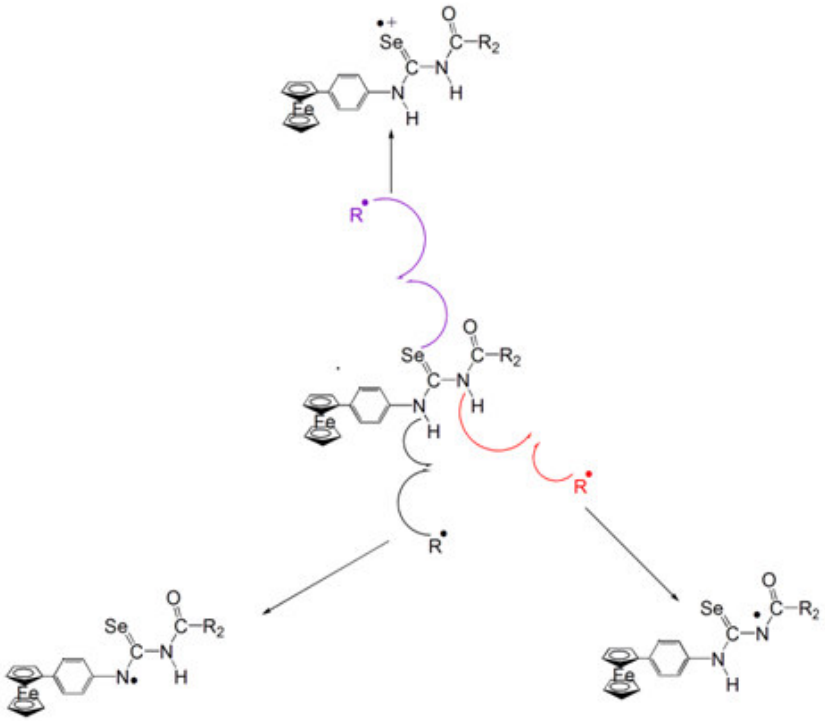

Chart 3. CD values of previously reported selenoureas.

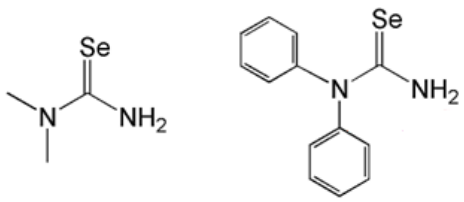

109 ± 17μM 22 ± 0.6 μM

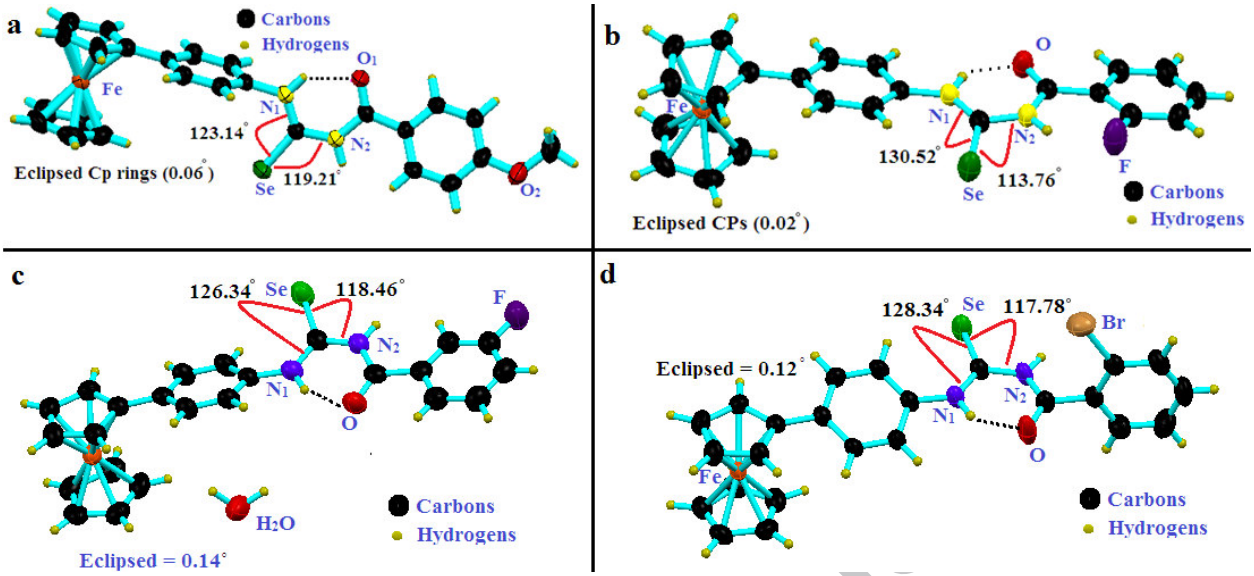

Figure 1. Single crystal XRD structures of a) 1-(4-methoxybenzoyl)-3-(4-ferrocenylphenyl)selenourea, b) 1-(2-fluorobenzoyl)-3-(4-ferrocenylphenyl)selenourea, c) 1-(3-fluorobenzoyl)-3-(4-ferrocenylphenyl)selenourea, d) 1-(2-bromobenzoyl)-3-(4-ferrocenylphenyl)selenourea.

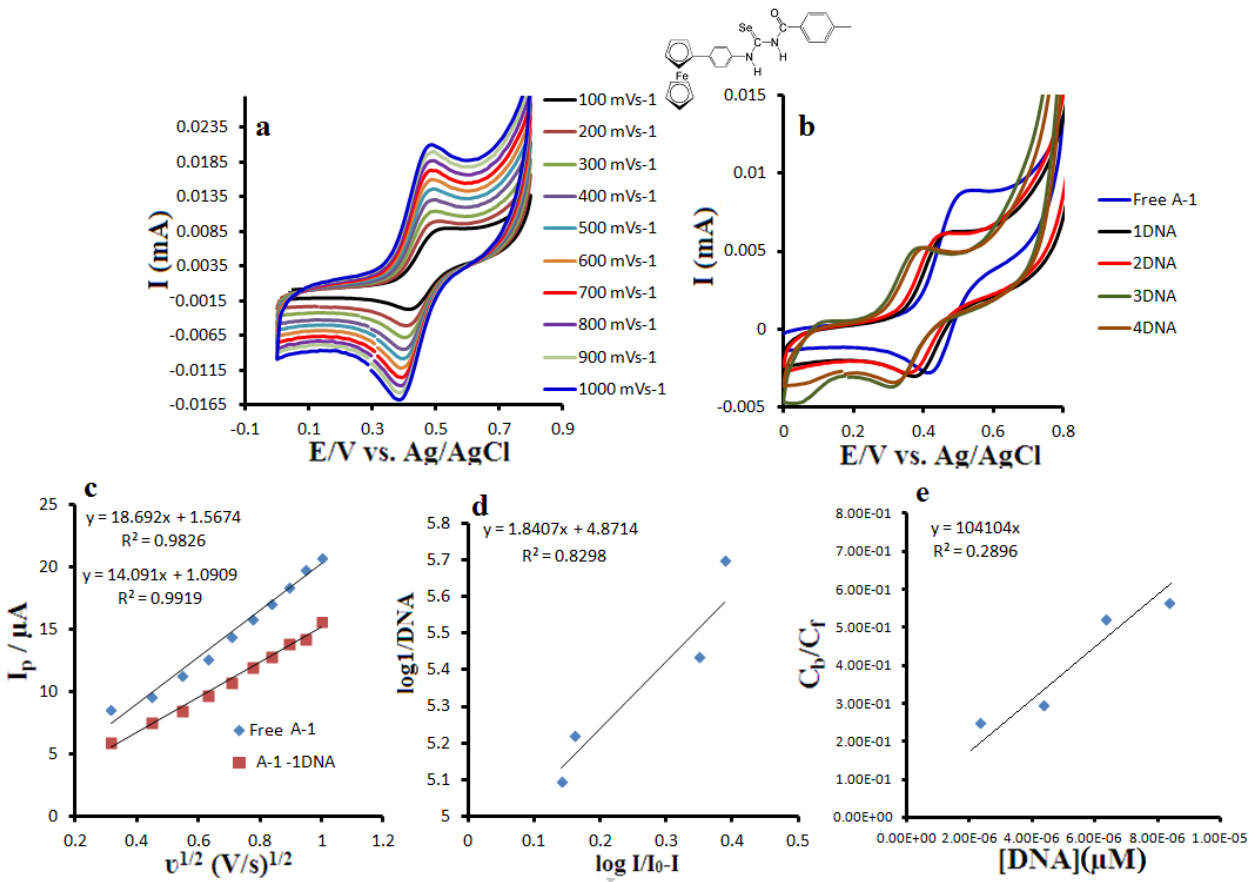

Figure 2. a) Cyclic voltammograms of 1 mM A-1 with 1 mL of 1.5 M KCl as a supporting electrolyte at different scan rates. b) Cyclic voltammograms of 1 mM A-1 with different DNA concentrations. c) Plots of I vs. $\upsilon^{½}$, for the determination of diffusion coefficients of A-1 (0 µM DNA) and 2 µM DNA bound A-1. d) Plot of log ($I/I_{\circ}$-I) vs. log (1/[DNA]) for determination of binding constant. e) Plot of C_b/C_f vs. [DNA] (µM) for determination of binding site size of 2-8 µM DNA concentrations.

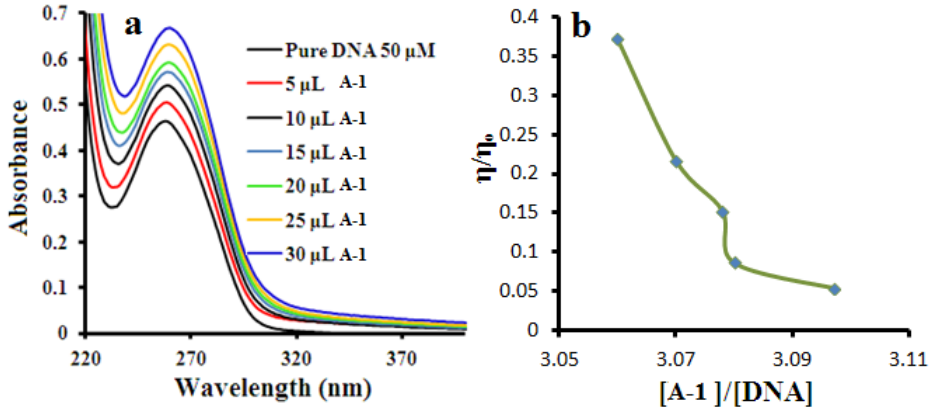

Figure 3. a) Plot of absorbance vs. wavelength of pure DNA and different DNA-A-1 adducts. b) Effect of increasing concentrations of A-1 on relative specific viscosity at 25 ± 1 °C.

Figure 4. %age DPPH scavenging by FIS using ascorbic acid as a positive control. General structure for the compounds is presented within the figure whereas different R groups provide different compounds in the series.

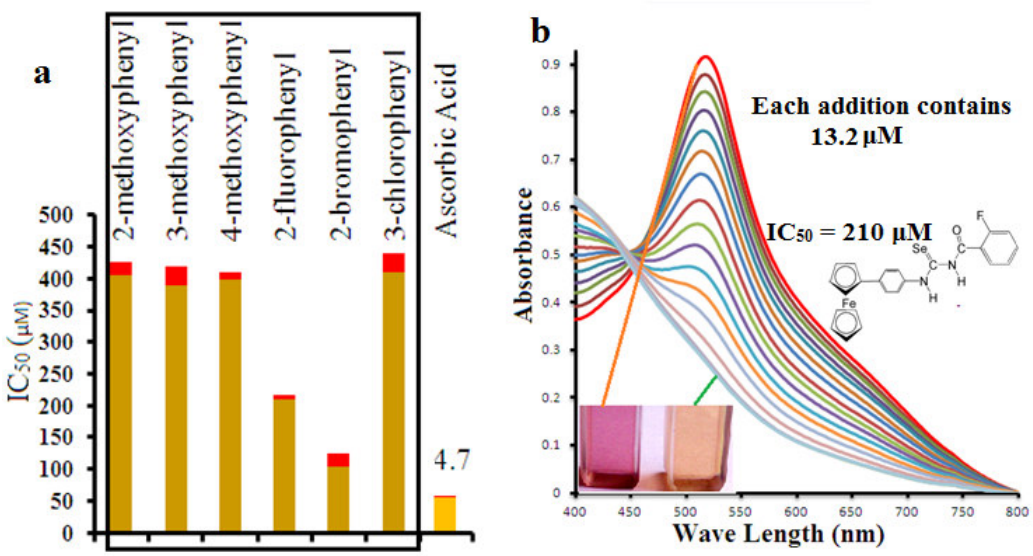

Figure 5. a) IC_{50} values of selected FIS. b) UV-vis spectra showing decrease in the absorbance of DPPH by the addition of FIS with the structure presented in the figure.

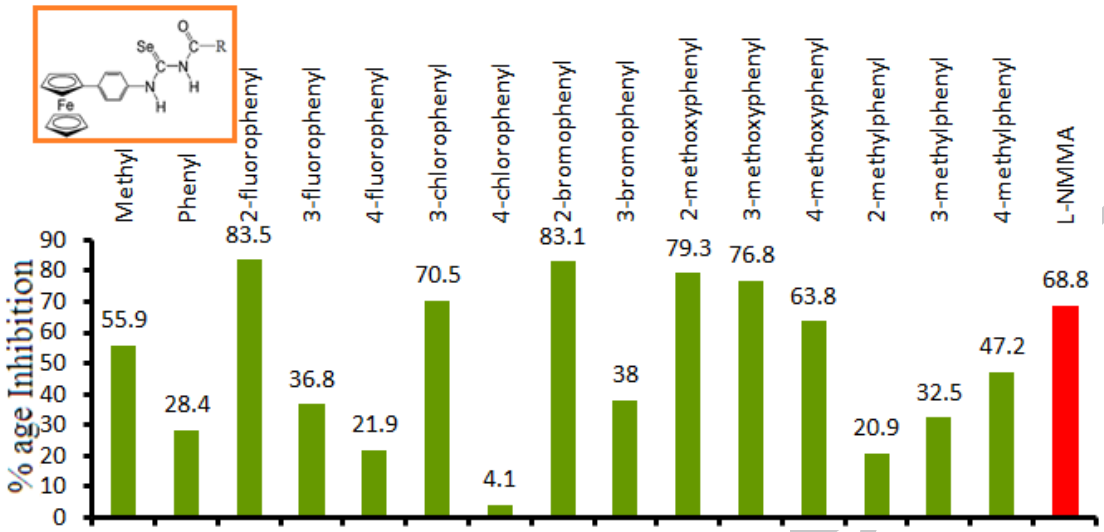

Figure 6. %age NO scavenging by synthesized FIS using LNMMA as a positive control. General structure for the compounds has been given below at the top whereas R groups are embedded within the figure.

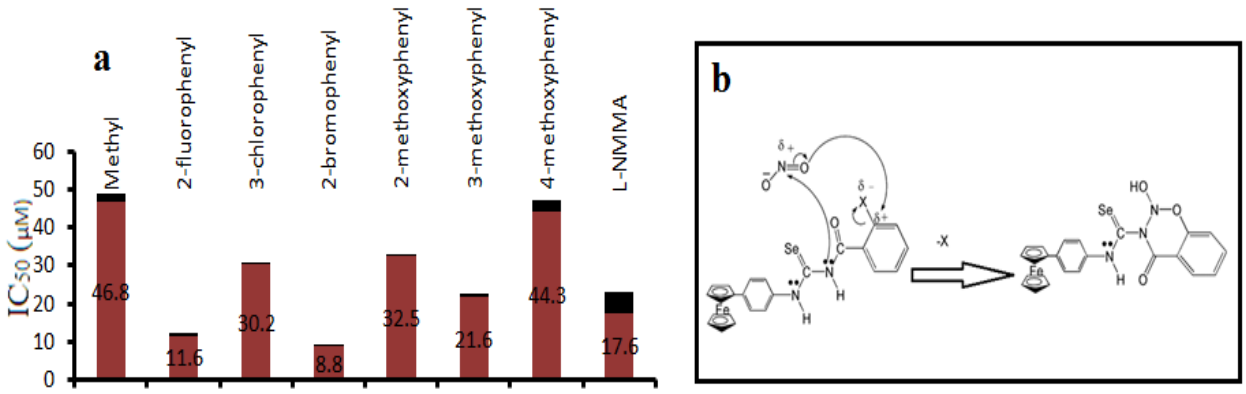

Figure 7. a) IC_{50} values of synthesized compounds using LNMMA as a positive control for NO scavenging. b) Possible byproduct formed by the interaction of ortho substituted derivatives with NO.

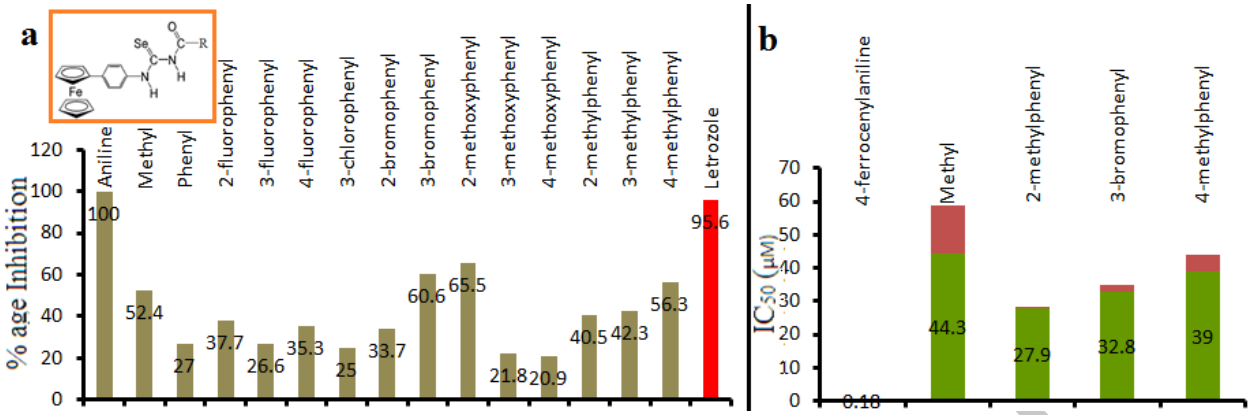

Figure 8. a) Aromatase inhibition activities of FIS using letrozole as a positive control. General structureof the compounds has been given above the figure whereas R groups are embedded within the figure. b) IC_{50} values for aromatase inhibition of synthesized FIS.

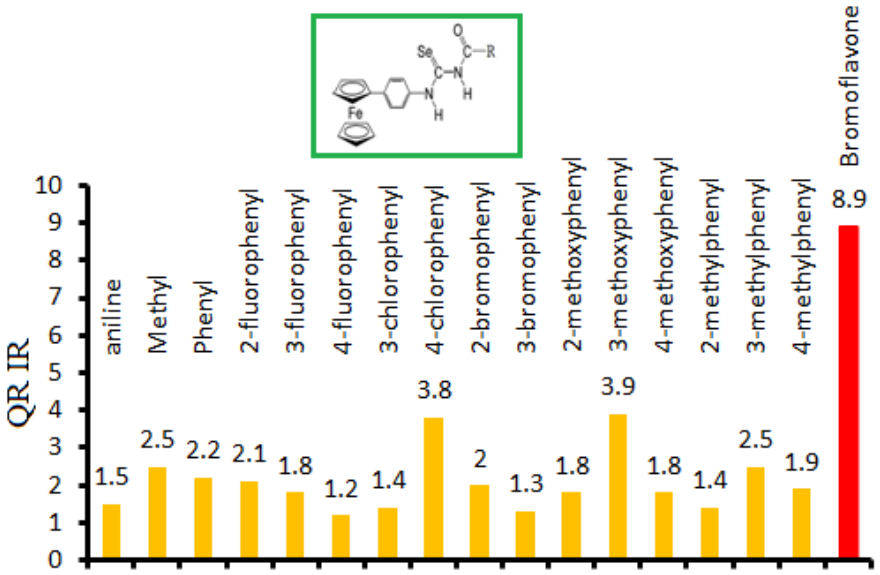

Figure 9. Quinone reductase induction activities of synthesized FIS. General structure of the compounds is presented above the figure whereas R groups are embedded within the figure.

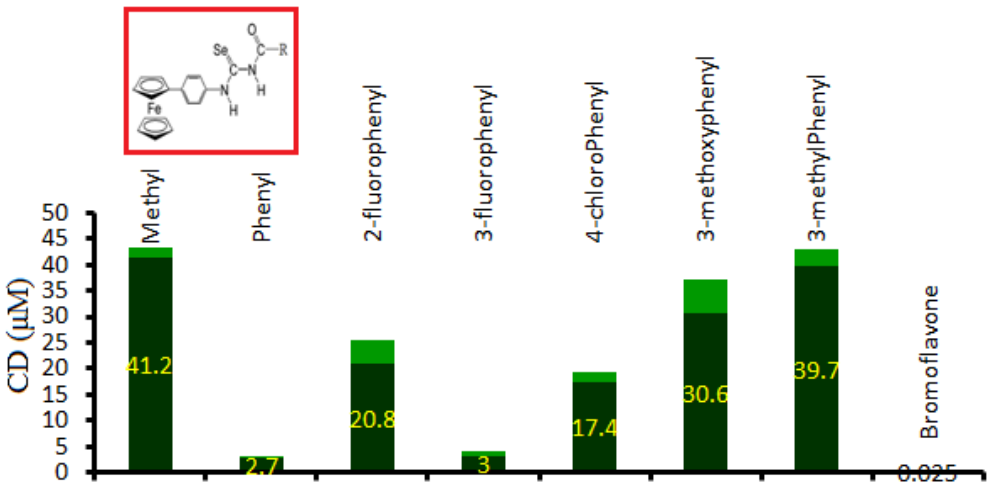

Figure 10. Concentration dose (CD) values of synthesized FIS. General structure of the compounds has been given above the figure whereas R groups are embedded within the figure.

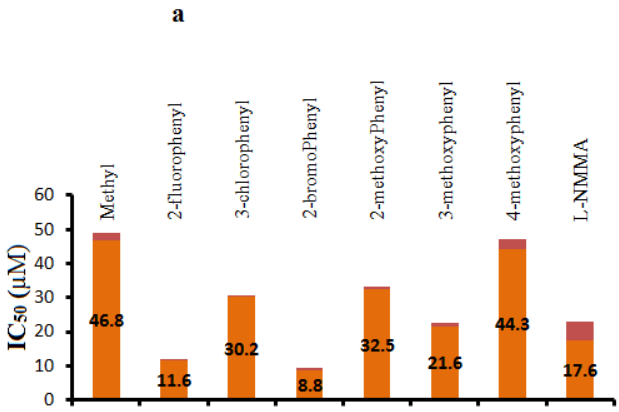
a
IC50 (µM)
60
50
40
30
20
10
0
Methyl
2-fluorophenyl
3-chlorophenyl
2-bromoPhenyl
2-methoxyPhenyl
3-methoxyphenyl
4-methoxyphenyl
L-NMMA
46.8
11.6
30.2
8.8
32.5
21.6
44.3
17.6

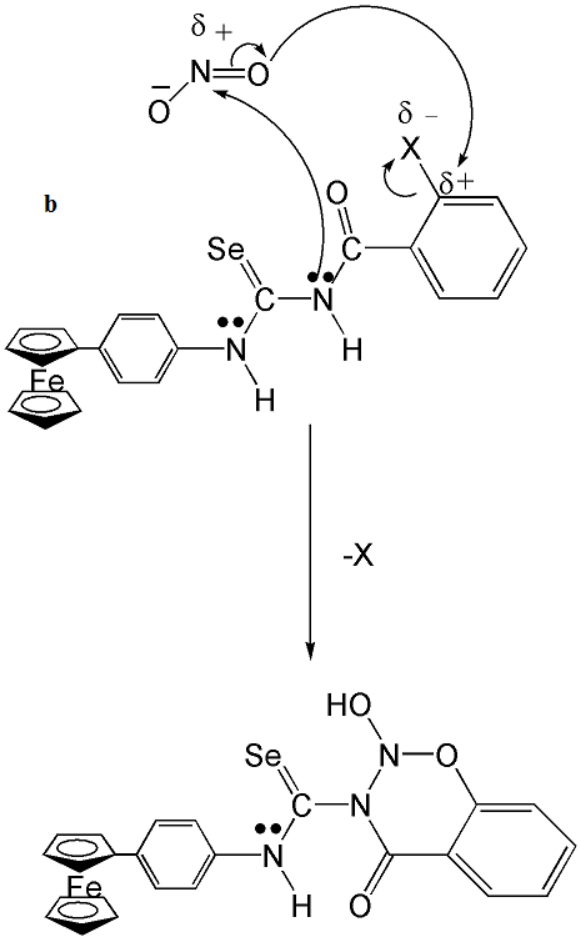
b
δ +
N
O
O
δ −
X
δ+
O
C
Se
C
N
H
N
H
Fe
-X
HO
N
O
Se
C
N
N
H
Fe
O

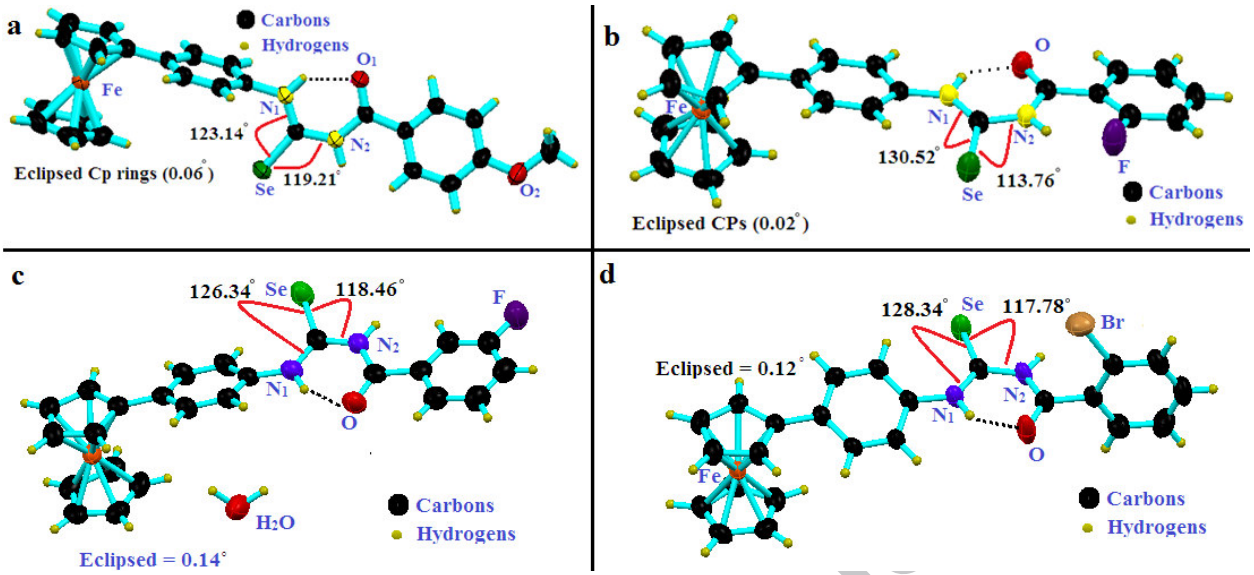

- Seventeen new ferrocene incorporated selenoureas (FIS) have been synthesized
- FIS have been characterized with FTIR, NMR, CHNS, and AAS.
- DNA binding, enzymatic and cytotoxic activities have been reported.